

Cancer Biology

Precision RNAi using synthetic shRNAmir target sites

Reviewed Preprint

Revised by authors after peer review.

About eLife's process

Reviewed preprint version 2

June 20, 2023 (this version)

Reviewed preprint version 1

March 3, 2023

Posted to bioRxiv

November 25, 2022

Sent for peer review

November 24, 2022

Thomas Hoffmann, Alexandra Hörmann, Maja Corcokovic, Jakub Zmajkovic, Matthias Hinterndorfer, Jasko Salkanovic, Fiona Spreitzer, Anna Köferle, Katrin Gitschtaler, Alexandra Popa, Sarah Oberndorfer, Florian Andersch, Markus Schäfer, Michaela Fellner, Nicole Budano, Jan G. Ruppert, Paolo Chetta, Melanie Wurm, Johannes Zuber , Ralph A. Neumüller 

Institute of Molecular Pathology (IMP), Campus-Vienna-Biocenter 1, 1030 Vienna, Austria • Vienna BioCenter PhD Program, Doctoral School of the University at Vienna and Medical University of Vienna, Vienna BioCenter (VBC), 1030 Vienna, Austria • Advantage Therapeutics GmbH, Karl-Farkas-Gasse 22, 1030 Vienna, Austria • Boehringer Ingelheim RCV GmbH & Co KG, Doktor-Boehringer-Gasse 5-11, 1120 Vienna, Austria • Medical University of Vienna, Vienna BioCenter, 1030 Vienna, Austria

 (https://en.wikipedia.org/wiki/Open_access)

 (<https://creativecommons.org/licenses/by/4.0/>)

Abstract

Loss-of-function genetic tools are widely applied for validating therapeutic targets, but their utility remains limited by incomplete on- and uncontrolled off-target effects. We describe artificial RNA interference (ARTi) based on synthetic, ultra-potent, off-target-free shRNAs that enable efficient and inducible suppression of any gene upon introduction of a synthetic target sequence into non-coding transcript regions. ARTi establishes a scalable loss-of-function tool with full control over on- and off-target effects.

eLife assessment

This manuscript describes a **valuable** method to study the mechanism of action of essential genes and novel putative drug targets. Evidence for the effectiveness of the system, which is based on engineering pre-validated targets for RNA-mediated knockdown into genes of interest, is **compelling**, and the method should find use as an orthogonal method for generating gene specific knockdowns.

Introduction

Drug development is guided by genetic loss-of-function (LOF) experiments that validate a therapeutic target, study its general and disease-specific functions, and thereby model and benchmark expected activities of inhibitory molecules. Applied genetic tools include RNAi, CRISPR/Cas9, and site-specific recombination technologies such as the Cre-Lox or Flp-FRT systems^{1,2}. While these technologies have undoubtedly revolutionized genetic screening, target identification and validation, each method is associated with drawbacks that limit the usability for certain aspects of target validation. Specifically, RNAi is prone to off-target effects³⁻⁵ and insufficient knock-down levels, while CRISPR/Cas9-based methods are associated with off-target effects and incomplete LOF across cell populations. These

limitations are particularly problematic for candidate targets in oncology, which should ideally be validated genetically in cancer cell lines and tumor models *in vivo*. In both cases, insufficient LOF or off-target effects can lead to far-reaching misconceptions about target suppression effects. Outgrowth of wild-type clones that retain gene function upon CRISPR- and recombination-based gene editing can result in transient phenotypes that complicate data interpretation. Similarly, insufficient knock-down or uncontrolled off-target effects induced by RNAi can lead to an unjustified de-prioritization or pursuit of candidate targets, respectively. Prior to initiating the time- and resource-intensive process of drug development, more informative target validation assays would be highly desirable.

Results

To develop such an assay system, we reasoned that instead of using gene-specific LOF triggers for every new candidate gene, the expression of any gene could be efficiently suppressed by engineering the target site of a pre-validated, highly potent, synthetic short-hairpin RNA (shRNA) into its exonic sequence (Figure 1A). Besides ensuring efficient target knockdown in a highly standardized manner, such an approach would also provide control over off-target activities through expressing the shRNA side-by-side in target-site engineered and wildtype cells. This approach leaves the genome engineering procedure, needed to integrate the pre-validated artificial RNA interference (ARTi) target site into a gene of interest, as the only potential source of off-target effects. As suitable RNAi system, we chose optimized micro-RNA embedded shRNAs (shRNAmirs) in the miR-E backbone⁶, which do not interfere with endogenous miRNA processing⁷ and can be expressed from tet-responsive elements and other Pol-II promoters in the 3'-UTR of fluorescent reporter genes, thus providing a versatile system for inducible RNAi⁸. To identify potent ARTi sequences with minimal off-target activity, we analyzed the nucleotide composition of shRNAs that reach exceptionally high performance scores in common shRNA design algorithms⁹ and of miRNA seed sequences with exceptionally low off-target scores according to siSPOTR¹⁰. By merging nucleotide biases identified in both analyses, we derived a 22-nt base composition matrix for the design of ARTi shRNAmirs (TTCGWWNNNAHHWWCATCCGGN; W = A/T, H = A/T/C; N = A/T/G/C) (Figure 1B; Figure 1 - figure supplement 1A,B). To further reduce possible off-target effects, we eliminated all shRNAs whose extended seed sequence (guide positions 2-14) had a perfect match in the human or mouse transcriptome and, finally, selected six top-scoring ARTi predictions for experimental validation.

Design and selection of ARTi-shRNAmirs

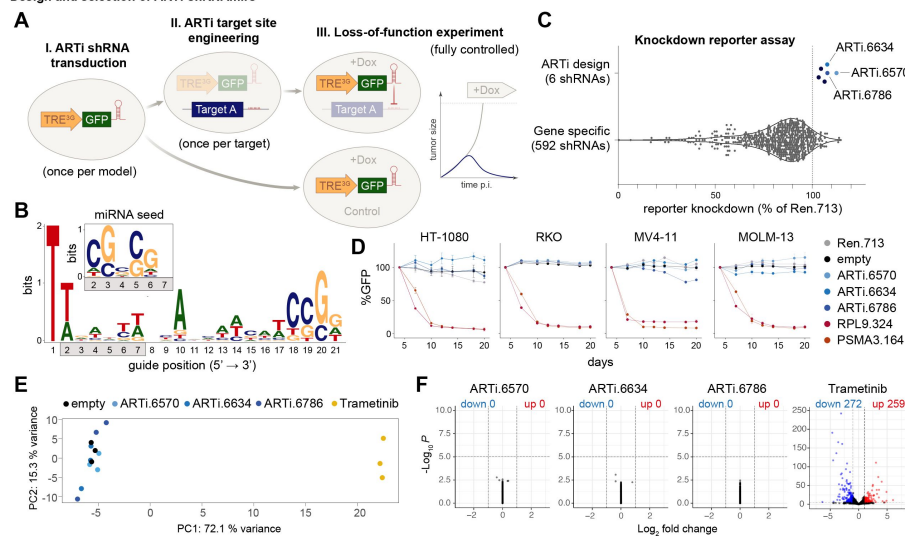


Figure 1:

Design and selection ARTi-shRNAmirs.

A, Schematic outline of the ARTi approach. **B**, Sequence logo (<https://weblogo.berkeley.edu>) displaying nucleotide position biases of 2161 shRNAs with exceptionally high DSIR scores (>105). Inlay depicts miRNA seed sequence biases. **C**, Reporter assay comparing gene-specific shRNAs to ARTi-shRNAmirs. **D**, Competitive proliferation assays in human cell lines after transduction with ARTi-shRNAmirs, neutral (shRen.713) and essential control

shRNAs (shRPL9.324 or shPSMA3.164). **E**, Principal component (PC) analysis of gene expression profiling upon stable expression of indicated shRNAs or treatment with MEK inhibitor (trametinib) in RKO cells. **F**, Volcano plots visualizing de-regulated genes upon expression of indicated shRNAs and trametinib treatment in RKO cells, compared to empty vector control.

We tested these ARTi-shRNAmirs using an established knockdown reporter assay⁶ for their ability to suppress expression of a GFP transgene that harbors the respective target sites in its 3'-UTR. In all six cases, ARTi-shRNAmir matched or outperformed previously validated highly potent shRNAmirs targeting Renilla luciferase or PTEN⁶ (Figure 1 - figure supplement 1C). We compared these results to a panel of 592 gene-specific shRNAs that were tested using the same assay and found that ARTi-shRNAmirs ranked among top-performing shRNAmirs overall (Figure 1C). Next, we selected the three top-performing ARTi-shRNAmirs and evaluated possible off-target activities using competitive proliferation assays and transcriptome profiling. ARTi-shRNAmir expression had no effects on proliferation or survival in four human and three mouse cell lines (Figure 1D; Figure 1 - figure supplement 1D), with the exception ARTi.6634 and ARTi.6786, which induced a mild fitness defect in the murine leukemia cell line RN2 and MV4-11 respectively. In contrast to effects of a MEK inhibitor trametinib, which we included as a positive control, stable expression of ARTi-shRNAmirs had only marginal effects on the transcriptome in two commonly used human cell lines (Figure 1E,F; Figure 1 - figure supplement 1E,F) and no effect in proliferation assays (Figure 1 - figure supplement 1G), indicating that they do not trigger major off-target effects, even in the absence of their respective target site. Together, these studies established a set of highly potent, off-target-free ARTi-shRNAmirs, among which we selected ARTi.6570 (ARTi-shRNAmir) for further investigations.

To establish ARTi as a method for target validation, we performed ARTi-based LOF experiments in cancer cell lines and xenograft models for three prominent oncology targets: EGFR and KRAS, which act as driving oncogenes in various cancer types^{11,12}, and STAG1, which has been identified as a synthetic lethal interaction with recurrent LOF mutations of STAG2¹³⁻¹⁶. To establish an ARTi-repressible version of oncogenic EGFR^{del19}, we cloned ARTi-shRNAmir target sequences into an expression construct encoding EGFR^{del19} fused to dsRed (Figure 2A), which rendered Ba/F3 cells cytokine-independent and sensitive to EGFR inhibition (Figure 2 - figure supplement 2A). We introduced this construct into human

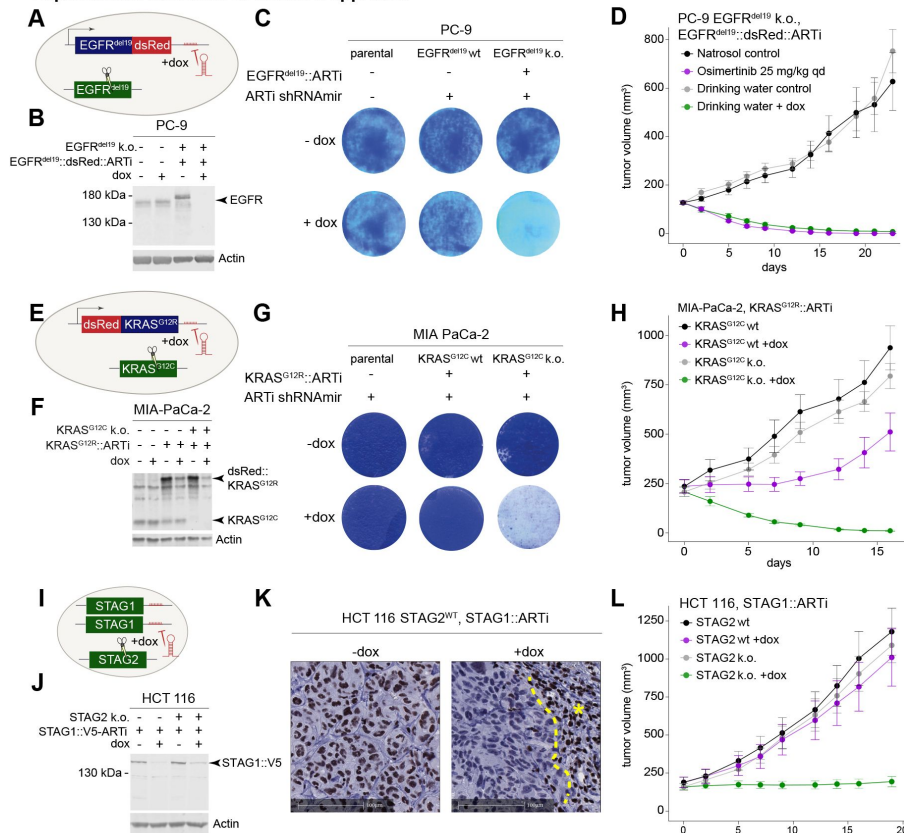
EGFR^{del19}-dependent PC-9 lung adenocarcinoma cells and subsequently knocked out the endogenous *EGFR* gene. The EGFR^{del19}::V5::dsRed::ARTi transgene fully rescued the loss of endogenous EGFR^{del19}, while doxycycline (dox)-induced expression of the ARTi-shRNAmir (ARTi.6570) strongly inhibited proliferation of PC-9 cells and triggered a near-complete suppression of the EGFR^{del19}::V5::dsRed::ARTi protein (Figure 2B,C; Figure 2 – figure supplement 2B). Consistently, in RNA-sequencing we observed an almost complete drop of reads mapping to the codon-optimized EGFR^{del19}::V5::dsRed::ARTi transgene upon dox-inducible expression of the ARTi-shRNAmir, as well as a downregulation of *DUSP6* and other canonical targets of RAF-MEK-ERK signaling, which acts as key effector pathway of EGFR^{del19} (Figure 2 – figure supplement 2C-E).

Figure 2:

Experimental validation of the ARTi approach.

A, Schematic of EGFR^{del19}::V5::dsRed::ARTi engineering in PC-9 cells. Blue color denotes overexpressed ARTi variant. Green denotes endogenous gene. **B**, Western Blot demonstrating knock-down of EGFR^{del19}::V5::dsRed::ARTi. Western Blot is a representative example of three independent biological repeat experiments. **C**, Proliferation assay and crystal violet staining of parental and engineered PC-9 cells in absence or presence of dox. Crystal violet staining is a representative example of two independent biological repeat experiments. **D**, *In vivo* experiment comparing dox-induced EGFR^{del19}::V5::dsRed::ARTi knockdown to pharmacological EGFR^{del19} inhibition. Mean tumor volume and +/- s.e.m. is plotted for

Experimental validation of the ARTi approach



all *in vivo* experiments. **E**, Schematic of MIA PaCa-2 engineering. Blue color denotes overexpressed ARTi variant. Green denotes endogenous gene. **F**, Western blot for KRAS and Actin in indicated engineered MIA PaCa-2 cells in the presence and absence of dox. Western Blot is a representative example of two independent biological repeat experiments. **G**, Proliferation assay and crystal violet staining of parental and engineered MIA PaCa-2 cells in absence or presence of dox. Crystal violet staining is a representative example of two independent biological repeat experiments. **H**, Growth curves of tumors implanted with engineered MIA PaCa-2 cells in absence and presence of dox. *In vivo* **I**, Schematic of C-terminal endogenous tagging of STAG1. Green color denotes endogenous genes. **J**, Western Blot demonstrating knock-down of STAG1-ARTi. Western Blot is a representative example of three independent biological repeat experiments. **K**, Immunohistochemistry staining of STAG1 in engineered HCT 116 cells in absence and presence of dox. Asterisk marks an area of murine fibroblasts that serve as an internal positive control. **L**, Growth curves of tumors implanted with engineered HCT 116 cells in the absence and presence of dox.

To evaluate whether ARTi can recapitulate drug activities *in vivo*, we xenotransplanted *EGFR^{del19}::V5::dsRed::ARTi* engineered PC-9 cells harboring the dox-inducible ARTi-shRNAmir and treated recipient mice upon tumor formation with either dox or the clinically approved EGFR inhibitor Osimertinib. Dox-induced expression of the ARTi-shRNAmir led to rapid and durable tumor regression that was indistinguishable from the effects of Osimertinib (Figure 2d) and not observed in parental PC-9 cells that lack the ARTi target site (Figure 2 – figure supplement 2F). We therefore conclude that ARTi-induced phenotypes are to be attributed to on-target effects that predict the activity of advanced small-molecule inhibitors *in vivo*.

In a second study, we used ARTi to investigate *KRAS^{G12R}*, an oncogenic *KRAS* variant with no available *in-vivo* compatible inhibitors. To establish a suitable *KRAS^{G12R}*-driven model, we engineered a *dsRed::KRAS^{G12R}-ARTi* transgene and the dox-inducible ARTi-shRNAmir into *KRAS^{G12C}*-dependent MIA PaCa-2 pancreatic adenocarcinoma cells and subsequently knocked out endogenous *KRAS* alleles (Figure 2E; Figure 2 – figure supplement 3A). As expected, switching the driving oncogene from *KRAS^{G12C}* to *KRAS^{G12R}* rendered MIA PaCa-2 cells resistant to the *KRAS^{G12C}* inhibitor AMG-510^{17–19} (Figure 2 – figure supplement 3B). ARTi-shRNAmir induction led to strong suppression of *dsRed::KRAS^{G12R}* expression at the mRNA and protein level (Figure 2F; Figure 2 – figure supplement 3C,D) and marked anti-proliferative effects (Figure 2G). In xenograft experiments, ARTi-mediated suppression of *KRAS^{G12R}* led to full tumor regression in the absence of *KRAS^{G12C}* (Figure 2H), while tumors harboring both oncogenic *KRAS* alleles only displayed a delay in tumor progression, suggesting that both oncogenes contribute to tumor growth *in vivo*.

To evaluate STAG1 as synthetic-lethal dependency that is relevant in wide range of STAG2-deficient cancers (Figure 2 – figure supplement 4A)^{13–16}, we engineered an isogenic pair of STAG2-wildtype and -deficient HCT 116 colon carcinoma cells and homozygously inserted ARTi target sites (besides an AID::V5 tag; explained in the materials and methods section) into the 3'-UTR of endogenous *STAG1* (Figure 2I). Western blotting confirmed the knockout of *STAG2*, the insertion of the targeting cassette into the *STAG1* locus, and potent suppression of *STAG1* following dox-induced ARTi-shRNAmir expression (Figure 2J,K; Figure 2 – figure supplement 4B). Suppression of *STAG1* in STAG2-deficient HCT 116 cells impaired their proliferation *in vitro* (Figure 2 – figure supplement 4C) and the progression of xenografted tumors *in vivo* (Figure 2L), while dox-induced expression of the ARTi-shRNAmir had no anti-proliferative effects in the presence of *STAG2*.

Discussion

Together, these studies establish ARTi as a versatile and precise LOF method for target validation in oncology and beyond. Instead of designing gene-specific LOF reagents that remain prone to off-target effects, ARTi involves a simple, highly standardized experimental procedure that provides full control over on- and off-target effects and can be applied to any coding and non-coding gene. In cells that are pre-engineered to express the dox-inducible ARTi-shRNAmir, candidate genes can be converted into ARTi target genes and subsequently evaluated head-to-head in a highly standardized manner, either through knocking in ARTi target sites into endogenous loci or through knock-out rescue approaches. Placement of ARTi target sites in non-coding transcript regions leaves the endogenous target protein unaltered, which is a key advantage over chemical-genetic LOF methods relying on the introduction of degron tags^{20,21}. Targeting endogenously engineered ARTi target sites through tetracycline (Tet)-inducible ARTi-shRNAmir expression enables inducible, titratable, and likely reversible (not tested in this study) LOF perturbations of candidate genes without altering their

endogenous transcriptional regulation, which is not possible using conventional Tet-expression systems. In principle, by engineering multiple target sites in the same cell, ARTi enables combinatorial LOF perturbations, e.g. for modeling synergistic target interactions, without multiplying the risk for off-target effects. Although ARTi requires the design of gene-specific sgRNAs and genome engineering steps that can be non-trivial, the method enables researchers to reach well-interpretable, comparable, and unambiguous experimental results that can guide larger investments in targets of high medical interest. Beyond providing a scalable method for early target validation, we foresee that ARTi can be used to establish on-target benchmark phenotypes for guiding the development and optimization of inhibitory molecules.

Figure Legends

Figure 1 – figure supplement 1: Design and selection ARTi-shRNAmirs. **A**, Sequence logo displaying nucleotide position biases of seed sequences (guide position 2-8) with the lowest off-target score in siSPOTR analysis (top 1%). **B**, Sequence logo displaying position biases in sequences from a that harbor a T in guide position 2. **C**, Knockdown efficiency of ARTi-shRNAmirs. Flow cytometric quantification of GFP knockdown efficiency in immortalized MEFs two days after transduction with indicated ARTi-shRNAmir or control shRNAs. Percent knockdown is normalized to shRen.713 control. shRen.660 served as a neutral control whose target site was not included in the reporter. Red asterisks indicate ARTi-shRNAmirs that were selected for follow-up studies. **D**, Toxicity of ARTi-shRNAmirs. Competitive proliferation assays of three murine cell lines after transduction with ARTi-shRNAmirs, shRen.713 or shMyc.1834 control, showing the relative fraction of shRNA-expressing cells at indicated time points following the initial measurement (day 4 after shRNA transduction). **E**, Principal component analysis of gene expression profiling in HT-1080 cells. Respective shRNAmirs and treatments are indicated in the respective colors. X-axis: principal component 1; Y-axis: principal component 2. **F**, Volcano plots visualizing de-regulated genes in HT 1080 cells. All shRNAmirs and treatments were tested against the empty vector control. X-axis: $-\log_{10}(\text{p-value})$; Y-axis: \log_2 fold change. **G**, Cell growth assay for ARTi-shRNAmir transduced cells and their parental controls in the presence and absence of dox.

Figure 2 – figure supplement 1: Validation of ARTi *in vitro* and *in vivo* - EGFR. **A**, Functional validation of the EGFR^{del19} construct in Ba/F3 cells. Provided are GI₅₀ values (nM) for indicated conditions and compounds (parental cells IL-3 dependent; other cells dependent on transgenes (no IL-3)). Numbers represent GI₅₀ value calculated from three technical repeats. Three biological repeat experiments were conducted, and one representative experiment is shown in panel A. **B**, Western Blot analysis confirming expression of EGFR^{del19}::V5::dsRed::ARTi constructs, knockout of endogenous EGFR and dox-induced knockdown or EGFR^{del19}::V5::dsRed::ARTi. Western Blot is a representative example of three independent biological repeat experiments. **C**, Expression levels (y-axis: normalized counts) of the EGFR^{del19}::V5::dsRed::ARTi construct in parental and engineered PC-9 cells after 4 and 8 days of dox treatment or no treatment. Individual datapoints of three biological replicates overlay the boxplots. **D**, Expression levels (y-axis: normalized counts) of the MAPK target gene *DUSP6* in parental and engineered PC-9 cells after 4 and 8 days of dox treatment or no treatment. Individual datapoints of three biological replicates overlay the boxplots. **E**, Heatmap visualizing the gene expression changes in MAPK pathway target and ERBB genes in engineered cells in the presence and absence of dox. **F**, *In vivo* experiment comparing dox-induced expression of the ARTi-shRNAmir to drinking water control in PC-9 parental cells. Lines connect mean tumor volume data and +/- s.e.m..

Figure 2 – figure supplement 2: Validation of ARTi *in vitro* and *in vivo* - KRAS. **A**, Schematic of MIA PaCa-2 genome engineering. **B**, AMG-510 GI₅₀ values in MIA PaCa-2 parental and engineered cells. Numbers represent GI₅₀ value calculated from three technical repeats. Three biological repeat experiments were conducted, and one representative experiment is shown in panel B. **C**, Expression levels (y-axis: normalized counts) of the dsRed::KRAS^{G12R} transgene in parental and engineered MIA PaCa-2 cells after 4 and 8 days of dox treatment or no treatment. Individual datapoints of three biological replicates overlay the boxplots. **D**, Western blot for KRAS (green) and Actin (magenta) (upper plot) and dsRed (green) and Actin (magenta) (bottom plot) for indicated engineered MIA PaCa-2 cells in the presence and absence of dox. Western Blot is a representative example of three independent biological repeat experiments.

Figure 2 – figure supplement 3: Validation of ARTi *in vitro* and *in vivo* – STAG1. **A**, Schematic of synthetic lethal interaction between STAG1 and STAG2. Cells survive loss of either paralog but are incapable of growing upon combined loss of STAG1 and STAG2. **B**, Western blot confirmation of STAG2 knockout and ARTi-shRNAmir induced knockdown of endogenous STAG1::V5::ARTi. Western Blot is a representative example of three independent biological repeat experiments. **C**, Proliferation assay of ARTi engineered HCT 116 cells *in vitro*, visualized by crystal violet staining following a 9-day dox or control treatment. Staining is a representative example of three independent biological repeat experiments. **D**, Quantification of nuclear Stag1 level (Figure 2k) using engineered HCT 116 cells in an *in vivo* xenotransplantation experiment the control group (-dox) and doxycycline (+dox) treated group.

Figure 2 – source data 1. Original blots for Figure 2B and Figure2 - figure supplement 1B.

Figure 2 – source data 2. Original blots for Figure 2F.

Figure 2 – source data 3. Original blots for Figure 2J.

Figure 2 – figure supplement 2 – source data 1. Original blots for Figure2 - figure supplement 2D.

Figure 2 – figure supplement 3 – source data 1. Original blots for Figure2 - figure supplement 3B.

Material and Methods

Design and cloning of ARTi shRNAs

To design pairs of artificial shRNAs and matching target sites that trigger effective and selective target suppression with minimal off-target effects, nucleotide composition of shRNAs that reach exceptionally high performance scores in a well-established siRNA prediction tool (DSIR=Designer of Small Interfering RNA⁹) and contain no A or T in guide position 20 to eliminate shRNAmirs that produce RISC-loadable small RNAs from the passenger strand were analyzed. To establish criteria for ARTi design, siRNA predictions for the human and mouse genome were retrieved from DSIR⁹ using default parameters. Top scoring predictions (DSIR score > 105) harboring G or C in position 20 were analyzed for nucleotide biases, which were used to define basic design criteria at the 5'-end the 3'-half. Next, possible off-targets were minimized using siSPOTR¹⁰, an siRNA-based prediction tool that assesses off-target potential of different siRNA seed sequences (guide positions 2-8) in the human and mouse genome. Seed sequences with the lowest predicted off-target activity

(top 1%) showed biases for C and/or G in guide positions 2-6, but 23% contained a T at the 5' end of the seed sequence that is required in our design (Fig. 1b). Among these, we observed particularly strong biases for CG in the following two positions (Fig. 1b), which were found in 73% of all seed sequences harboring a 5' T. Overall, 17% of all top-scoring seed sequences harbored TCG at their 5' end, making it the second most common triplet (after CGC, which was found in 20%). Based on these analyses, we fixed the first 4 nucleotides of the guide to TTCG. For the following positions we reasoned that introducing additional GC biases would destroy 5'-3' asymmetry of small RNA duplexes that is critically required for efficient RISC loading. To maintain sufficient asymmetry, we therefore decided to bias the next 3 positions towards A or T, which in most positions is in alignment with nucleotide biases associated with knockdown efficacy.

For the remaining sequence 3' of the seed region, we adhered to nucleotide features associated with knockdown efficacy based on our DSIR analysis, which are remarkably prominent and cannot all be explained through established processing requirements. Altogether, this established a 22-nt matrix for the design of ARTi shRNAmirs (TTCGWWNNAAHHWWCATCCGNN; W = A/T, H = A/T/C; N = A/T/G/C). In a last step, we further reduced possible off-target effects by eliminating all guides whose extended seed sequence (guide positions 2-14) had a perfect match in the human or mouse transcriptome and, finally, selected the following six top-scoring ARTi predictions for experimental validation:

ARTi.6588 – target site: TCCGGATGAAGTTTATATCGAA / shRNAmir (97mer):
TGCTGTTGACAGTGAGCGCCCGGATGAAGTTTATATCGAATAGTGAAGCCACAGATGTATTCGATATA
AACTTCAT CCGGATGCCTACTGCCTCGGA

ARTi.6570 – target site: TCCGGATGATATTGTTATCGAA / shRNAmir (97mer):
TGCTGTTGACAGTGAGCGCCCGGATGATATTGTTATCGAATAGTGAAGCCACAGATGTATTCGATAAC
AATATCAT CCGGATGCCTACTGCCTCGGA

ARTi.6634 – target site: TCCGGATGATGTTTAAATCGAA / shRNAmir (97mer):
TGCTGTTGACAGTGAGCGCCCGGATGATGTTTAAATCGAATAGTGAAGCCACAGATGTATTCGATTAA
AACATCAT CCGGATGCCTACTGCCTCGGA

ARTi.6786 – target site: TCCGGATGATATTGTATACGAA / shRNAmir (97mer):
TGCTGTTGACAGTGAGCGCCCGGATGATATTGTATACGAATAGTGAAGCCACAGATGTATTCGTATAC
AATATCAT CCGGATGCCTACTGCCTCGGA

ARTi.6834 – target site: TCCGGATGATATTGCATACGAA / shRNAmir (97mer):
TGCTGTTGACAGTGAGCGCCCGGATGATATTGCATACGAATAGTGAAGCCACAGATGTATTCGTATGC
AATATCAT CCGGATGCCTACTGCCTCGGA

ARTi.6516 – target site: TCCGGATGAAGTTTAAATTCGAA / shRNAmir (97mer):
TGCTGTTGACAGTGAGCGCCCGGATGAAGTTTAAATTCGAATAGTGAAGCCACAGATGTATTCGAATT
AACTTCAT CCGGATGCCTACTGCCTCGGA

The following ARTi target sequences were used for experimental validation studies:
Insertion into the coding sequence before the STOP codon:

ATCCGGATGATATTGTATACGAATCCGGATGATATTGTTATCGAA (with the first “A” being inserted to retain the reading frame)

Insertion after the STOP codon:

TCCGGATGATATTGTATACGAATCCGGATGATGTTTAAATTCGAATCCGGATGATATTGTTATCGAA
shRNAs were ordered as single stranded DNA Ultramer oligonucleotides (Integrated DNA Technologies), amplified by PCR and cloned into different retroviral or lentiviral miRE/miRF

shRNAmir expression vectors (LT3GFPIR⁶) using EcoR/XhoI restriction digest or Gibson assembly.

Cell Culture

Human HCT 116 cells (ATCC: CCL-247) were cultured in RPMI 1640 medium (Thermo Fisher) and PC-9 cells in McCoy's 5A medium (Thermo Fisher), supplemented with 10% FBS and 1 x GlutaMAX (Thermo Fisher). RKO (ATCC: CRL-2577) and MOLM-13 cells (DSMZ: ACC 584) were cultured in RPMI 1640, supplemented with 10% FBS (Sigma-Aldrich), 4mM L-glutamine (Thermo Fisher), 1mM sodium pyruvate (Sigma-Aldrich), and penicillin/streptomycin (100 U ml⁻¹/100 µg ml⁻¹, Sigma-Aldrich). HT-1080 (ATCC: CCL-121) and LentiX lentiviral packaging cells (Clontech, cat. no. 632180) were cultivated in DMEM (Thermo Fisher) with 10% FBS, 4mM L-glutamine, 1mM sodium pyruvate, and penicillin/streptomycin (100 U ml⁻¹/100 µg ml⁻¹). MV4-11 cells (ATCC: CRL-9591) were cultured in IMDM with 10% FBS, 4mM L-glutamine, 1mM sodium pyruvate, and penicillin/streptomycin (100 U ml⁻¹/100 µg ml⁻¹).

Murine MLL-AF9^{OE}, Nras^{G12D} AML cells (RN2; Zuber et al. 2011) were cultured in RPMI 1640 medium supplemented with 10% FBS, 20 mM L-glutamine, 10 mM sodium pyruvate, 10 mM HEPES (pH 7.3), penicillin/streptomycin (100 U ml⁻¹/100 µg ml⁻¹), and 50 µM β-ME. *Kras*^{G12D}, *Trp53*^{-/-}, *MYC*^{OE} PDAC cells (EPP2), SV40 large T antigen immortalized mouse embryonic fibroblasts (RRT-MEF²²; and NIH/3T3 (ATCC: CRL-1658) were cultured in DMEM supplemented with 10% FBS, 20 mM glutamine, 10 mM sodium pyruvate, and penicillin/streptomycin (100 U ml⁻¹/100 µg ml⁻¹). MIA PaCa-2 (ATCC: CRL-1420) and GP2d (Ecacc: 95090714) cells were cultured in DMEM supplemented with 10% FBS. Ba/F3 (DSMZ: ACC300) cells were cultured in RPMI 1640 medium supplemented with 10% FBS, 10ng/ml IL-3 (R&D systems) and Ls513 cells were cultured in RPMI 1640 medium supplemented with 10% FBS. All cell lines were maintained at 37°C with 5% CO₂, routinely tested for mycoplasma contamination and authenticated by short tandem repeat analysis.

Reporter Assay

SFFV-GFP-P2A-Puro-ARTi-target sensor was cloned into pRSF91 retroviral plasmid²³ using Gibson assembly. RRT-MEFs were transduced with retroviruses expressing a GFP-reporter harboring the target sites for validated shRNAs and one ARTi-shRNA in its 3'-UTR. For each reporter cell line single cells were FACS-sorted into 96-well plates using a FACSaria III cell sorter (BD Bioscience) to obtain single-cell derived clones. These clones were transduced with retrovirus constructs in pSin-TRE3G-mCherry-miRE-PGK-Neo (TCmPNe) backbone expressing either the respective doxycycline (dox)-inducible ARTi shRNA or validated shRNAs and mCherry fluorescence marker. shRNA expression was induced with dox and GFP levels were quantified via flow cytometry 2 days post induction. Knockdown efficiency was calculated as 1 minus the ratio of mean GFP signal in mCherry⁺ (shRNA⁺) cells over mCherry⁻ cells and normalized to Renilla luciferase specific neutral control shRNA (Ren.713).

Competitive proliferation assay

To investigate the effect of ARTi constructs in the absence of the endogenous target gene, competitive proliferation assays were performed in several human and murine cell lines. Human HT-1080, RKO, MOLM-13, and MV4-11 cell lines were lentivirally transduced with shRNAmir expression constructs cloned into pRRL-SFFV-GFP-miRF-PGK-Neo (SGFN) backbone at 20-60% efficiency. Initial infection efficiency was determined at day 4 post transfection (day 0) by measuring GFP expression as a readout using iQue Screener Plus flow cytometer (IntelliCyt). Percentage of shRNA⁺ cells (GFP positive) was monitored by flow cytometry in regular intervals and results were normalized to day 0.

Human GP2d, Ls513, and MIA PaCa-2 cell lines were lentivirally transduced with shRNAmir constructs cloned into pRRL-TRE3G-GFP-miRE-PGK-Puro-IRES-rtTA3 backbone (LT3GEPIR, Addgene plasmid #111177). 500 cells were seeded in duplicates in 96-well plates and treated with 1 µg/ml dox for 9-10 days and analyzed with Incucyte (Sartorius). Untreated cells served as reference.

Murine NIH-3T3, EPP2 and RN2 cells were retrovirally transduced with shRNAmir constructs cloned into pMSCV-miR-E-PGK-Neo-IRES-mCherry backbone (LENC; Addgene plasmid #111163), and initial infection levels were determined by flow cytometry based on mCherry expression 4 days post transduction (day 0).

Crystal Violet staining

To visualize ARTi-shRNAmir's effect, crystal violet staining assays were performed. 25'000 HCT 116 cells and 15'000 PC-9 cells per well were seeded in a 6-well plate containing 2 mL tetracycline-free growth medium and 1 µg/mL dox. Medium was exchanged every 2-3 days. After 9 days, wells were washed with ice-cold PBS and subsequently stained with 1 mL of 2.3% crystal violet solution for 10 minutes. Subsequently, wells were washed with ultrapure water and dried overnight. Images were obtained with a scanner.

Transcriptional profiling

For the unbiased identification of ARTi shRNA off-targets, RKO and HT-1080 shRNA⁺ cells from the competition proliferative assay experiment were selected with Geneticin/G418 Sulfate (Gibco) for 7 days and checked for GFP expression. On day 7, one arm of the empty vector control group was treated with IC₅₀ concentration of trametinib (MedChem Express: HY-10999) for 24 hours based on the data in Genomics of Drug Sensitivity in Cancer (GDSC) database (<https://www.cancerrxgene.org>)²⁴. Subsequently, cells were trypsinized, washed with ice-cold PBS, pelleted and snap frozen. Total RNA was isolated using in-house magnetic beads kit and King Fisher Duo Prime Purification System (Thermo Fisher). NGS libraries were prepared with QuantSeq 3' mRNA-Seq Library Prep Kit (FWD) HT for Illumina (Lexogen) and UMI Second Strand Synthesis Module for QuantSeq FWD (Lexogen). Samples were sequenced on Illumina NovaSeq platform with 100bp single-read protocol.

Engineered MIA PaCa-2 and PC-9 cells were cultured in the presence of 1 µg/ml dox to induce expression of the ARTi shRNA. dox-containing media were replenished twice weekly and on day 4 and day 8 after the initial treatment. 2×10⁶ dox-treated and untreated control cells were harvested, washed with PBS, lysed, treated with DNase I (QIAGEN) and total RNA was extracted using the RNeasy Mini Kit (QIAGEN). NGS libraries were prepared as above. Samples were sequenced on an Illumina NextSeq 2000 platform with a 75bp protocol.

Bioinformatic analyses of 3' mRNA-Seq

For 3' mRNA-Seq reads derived from the human cell lines HT-1080 and RKO, the six nucleotide long 5' UMIs were attached to each read name with umi-tools (v1.0.0)²⁵. Subsequently, the UMIs plus the next four nucleotides (UMI spacer), as well as 3' adapters (stringency of 3) and bases with low quality (threshold of 25) were trimmed away using cutadapt (v1.18)²⁶ and its wrapper tool trimgalore (v0.6.2). Read quality control was performed with FastQC (v0.11.8). The remaining reads were sample-wise aligned to the human (GRCh38.p13; GCA_000001405.28) reference genome. Mapping and subsequent filtering of 3' UTR mapped reads was performed with slamdunk (v0.4.3)²⁷ in QuantSeq mode (slamdunk map -5 12 -n 100 -q). 3' UTR regions were assembled based on the description in

Muhar et al.²⁸. Aligned and filtered reads were deduplicated with umi-tools (v1.0.0) (2), based on the mapping coordinate and the UMI attached to the read name, prior to quantifying read abundances within 3' UTR regions using featureCounts (v2.0.1)²⁹. Differential expression analysis (DEA) was performed with DESeq2 (v1.30.1)³⁰ for each ARTi shRNA to empty vector control. Here, the number of up- and downregulated genes were calculated by filtering the DEA results for genes with a log2 fold-change ≥ 2 (up) or ≤ 2 (down) and a $-\log_{10}$ p-value ≥ 5 . Principal component analysis was performed on the 1000 most variable expressed genes with the prcomp function from the stats (v4.2.0) R package.

For transcriptional profiling of the human cell lines MIA PaCa-2 and PC-9, the genome reference file and annotations were constructed based on the GRCh38 assembly and the Ensembl 86 version, respectively. The sequences of the shRNA construct (ARTi.6570 (RN_v_76, RN_v_118)) as well as the EGFR^{del19}::V5::dsRed::ARTi (RN_v_108) and the dsRed::Linker::KRAS^{G12R}-ARTi (RN_v_287) were also included. Mapping of the sequencing reads derived from the human cell lines was performed with STAR (v2.5.2b)³¹ aligner allowing for soft clipping of adapter sequences. Quantification of read counts to transcript annotations was implemented using RSEM (v1.3.0)³² and featureCounts (v1.5.1)²⁹. Normalization of read counts and differential analysis was implemented with the limma³³ and voom³⁴ R packages.

Genome engineering of EGFR in PC-9 and Ba/F3

Genome engineering of PC-9 cells was done as previously described³⁵. In brief: PC-9_RIEN cells were transduced with an ecotropic pMSCV-EGFRdel19_V5_dsRed_ARTi-PGK-Blasticidin retrovirus cloned at GenScript and produced in Platinum E cells (Cell Biolabs) in the presence of 8 $\mu\text{g/mL}$ Polybrene (Merck Millipore). After 24 hours, stable transgenic cell pools were selected using 10 $\mu\text{g/mL}$ Blasticidin (Sigma-Aldrich). Subsequently, cells were diluted to obtain single cell clones. After 14 days of culture, single cell-derived colonies were transferred to 6-well plates and analyzed by Western Blot. Identified homozygous PC-9_EGFR^{del19}-ARTi clones were further engineered by cutting endogenous EGFR with a CRISPR all-in-one vector pX458_Exon20_gRNA TAGTCCAGGAGGCAGCCGAA (GenScript) using XtremeGENE 9 DNA transfection reagent (Roche) according to the protocol supplied by the vendor. 48 hours after transfection, GFP positive cells were sorted by FACS (SONY cell sorter S800Z) and diluted to obtain single cell clones. Positive clones, which contained only the exogenous EGFR^{del19}-ARTi, but not the endogenous EGFR, were identified by Western Blot. Next, the selected EGFR clone was transduced with a pantropic LT3GEPiR_Puro_ARTi-shRNA TTCGATAACAATATCATCCGGA retrovirus cloned at GenScript, China and produced via the Lenti-X Single Shot system (Clontech). 72 hours later, stable transgenic cell pools were selected using 0.5 $\mu\text{g/mL}$ Puromycin (Sigma-Aldrich). Following the selection, cells were diluted to obtain single cell clones. After 14 days of culture, single cell-derived colonies were transferred to 6-well plates and induced via 1 $\mu\text{g/mL}$ dox. Positive clones were characterized by a strong GFP-induction that was identified by flow cytometry.

Ba/F3 cells were transduced with an ecotropic pMSCV-EGFRdel19_V5_dsRed_ARTi-PGK-Blasticidin retrovirus cloned at GenScript and produced in Platinum E cells in the presence of 4 $\mu\text{g/mL}$ Polybrene. After 72 hours, stable transgenic cells were selected by using 50 $\mu\text{g/mL}$ Blasticidin, without adding IL-3.

Genome engineering of KRAS in MIA PaCa-2

MIA PaCa-2 ARTi-shRNAmir expressing cells were transduced with an ecotropic pMSCV-dsRed::KRAS^{G12R}-ARTi-PGK-Blasticidin retrovirus cloned at GenScript, China and produced in Platinum E cells in the presence of 8 $\mu\text{g/mL}$ Polybrene. After 24 hours, stable transgenic

cell pools were selected using 10 µg/mL Blasticidin. Subsequently, endogenous KRAS was knocked out by transient transfection of three gRNAs targeting exon 2 and the region containing the G12C variant (present in MIA PaCa-2 cells) were used in a co-transfection (gRNA#3: *GAATATAAACTTGTGGTAGT*; gRNA#6: *CTGTGGTAGTTGGACTTG*; gRNA#7: *GTAGTTGGAGCTTGTGGCGT*). Knockout clones were identified by the absence of the endogenous KRAS protein using Western Blot.

Genome engineering of STAG1/STAG2 in HCT 116

HCT 116 cell line was engineered by cutting STAG1 with gRNAs targeting the region close to the STOP codon. Guide RNAs *TTCTTCAGACTTCAGAACAT* or *CTGAAGAAAATTTACAAATC* were cloned into the pSpCas9(BB)-2A-GFP plasmid (pX458; Addgene plasmid 48138) and used in a co-transfection. Simultaneously, a STAG1_AID_V5_P2A_Blasti_STOP_ARTi repair template with 800bp of left and right homologous arms of the STAG1 genomic locus (in pUC57-Simple backbone) was transfected into HCT 116 cells using Lipofectamine 3000 transfection reagent (Thermo Fisher) according to the manufacturer's instructions. A stable transgenic cell pool was selected 48 hours after transfection using 5µg/ml Blasticidin and diluted to obtain single cell clones. Positive clones were identified by Western Blot.

Identified homozygous HCT 116_STAG1_ARTi clones were further engineered by disrupting STAG2 gene with a CRISPR all-in-one vector Hs0000077505_U6gRNA-Cas9-2A-GFP and Hs0000077502_U6gRNA-Cas9-2A-GFP, respectively. Cells were transfected using X-tremeGENE 9 DNA transfection reagent according to the manufacturer's instructions, sorted 48 hours post transfection for GFP positive cells and diluted to obtain single cell clones. Positive clones were identified by Western Blot.

Next, the selected HCT 116 clone was transduced with a pantropic LT3GEPiR_Puro_ARTi-shRNA *TTCGATAACAATATCATCCGGA* retrovirus cloned at GenScript, China and produced via the Lenti-X Single Shot system (Clontech). 72 hours later, stable transgenic cell pools were selected using 2 µg/mL Puromycin (SIGMA, P9620). Following the selection, cells were diluted to obtain single cell clones. After 14 days of culture, single cell-derived colonies were transferred to 6-well plates and induced via 1µg/ mL dox. Positive clones were characterized by a strong GFP-induction that was identified by flow cytometry.

Western Blot

The following primary antibodies were used for immunoblot analyses: EGFR (Cell Signaling, #4267); STAG1 (GeneTex, GTX129912); STAG2 (Bethyl, A300-159A); b-actin (Sigma, A5441); KRAS (LSbio, LS-C17566); V5 (Sigma, V8012). PC-9, MIA PaCa-2, and HCT 116 cell pellets harboring EGFR, KRAS, and STAG1/STAG constructs respectively were lysed in Triton X-100 lysis buffer, sonicated and stored at -80°C. For protein detection, the pellets were thawed on ice, followed by 15 minutes centrifugation at 13,000 rpm and 4°C. Further, cell lysates were loaded onto a pre-casted SDS-polyacrylamide gel (4-12%) and proteins were transferred onto a nitrocellulose or PVDF-membrane. Membranes were probed with the respective primary antibodies overnight. The next day, secondary antibodies conjugated with fluorescent dye were added and the proteins were detected by the Odyssey detection system.

Compound treatment

To investigate sensitivity to EGFR-targeting compounds, cell viability was determined using the Cell Titer Glo assay (Promega). For this purpose, 10 mM stock solutions in DMSO of afatinib³⁶, Osimertinib^{37,38 37} and poziotinib^{39,40} were used. 5'000 cells per well were seeded in 150µL of the medium in technical triplicates in 96-well plates and incubated at 37°C and

5% CO₂ for 5 hours, followed by the compound addition. Cells were treated with seven different concentrations of inhibitors in a serial eight-fold dilutions starting with the highest concentration of 3 μM. For comparability, DMSO normalization to the highest added volume was performed. Subsequently, cells were cultivated for 96 hours at 37°C and 5% CO₂. 50 μL of Cell Titer Glo reagent was added to each well, incubated for 10 minutes in the dark and luminescence was measured using the multilabel Plate Reader VICTOR X4. The measurement time was set to 0.2 seconds. Luminescence values relative to DMSO-treated cells were plotted in GraphPad Prism and fitted using nonlinear regression with a variable slope to calculate IC₅₀ values at 50% inhibition. MIA PaCa-2 KRAS G12C inhibitor (AMG-510)^{17–19} treatments were performed as described for EGFR with the following modifications: 2'000 cells per well, and 0.5nM–3μM concentration range of AMG-510.

***In vivo* experiments**

The PC-9 EGFR k.o., EGFR^{del19}::ARTi study was performed at the AAALAC accredited animal facility of CrownBio Leicestershire, UK. Female NSG® (NOD.Cg-PrkdcscidII2rgtm1wjl/SzJ) Crl mice were obtained from Charles River. Age of animals at study initiation was 7–8 weeks and had an acclimatization period of ≥14 days. Mice were groups housed in IVCs. The study complies with the UK Animals Scientific Procedures Act 1986 (ASPA) in line with Directive 2010/63/EU of the European Parliament and the Council of 22 September 2010 on the protection of animals used for scientific purposes.

All other *in vivo* experiments were performed at the AAALAC accredited animal facility of Boehringer Ingelheim RCV GmbH & CoKG. Female BomTac:NMRI-Foxn1^{nu} mice were obtained from Taconic Denmark at 6–8 weeks of age. After the arrival, mice were allowed to adjust to the housing conditions at least for 5 days before the start of the experiment. Mice were housed in pathogen-free and controlled environmental conditions (open cage housing), and handled according to the institutional, governmental and European Union guidelines (Austrian Animal Protection Laws, GV-SOLAS and FELASA guidelines).

Studies were approved by the internal ethics committee (called “ethics committee”) of Boehringer Ingelheim RCV GmbH & Co KG in the department of Cancer Pharmacology and Disease Positioning. Furthermore, all protocols were approved by the Austrian governmental committee (MA 60 Veterinary office; approval numbers GZ: 903122/2017/21 and GZ: 416181-2020-29).

To establish subcutaneous tumors, mice were injected with 2×10^6 HCT 116 in PBS, 5×10^6 MIA PaCa-2 in 1:2 Matrigel : PBS with 5% FBS or with 1×10^7 PC-9 cells in PBS with 5% FBS.

Tumor diameters were measured with a caliper three times a week. The volume of each tumor [in mm³] was calculated according to the formula “tumor volume = length * diameter² * π/6.” Mice were randomized into the treatment groups when tumor size reached between ~130 and 190 mm³. Group sizes were calculated for each tumor model based on tumor growth during model establishment experiments. A power analysis was performed using a sample size calculator (<https://www.stat.ubc.ca/~rollin/stats/ssize/n2.html>). For all models used in the studies, 10 mice per group were used. 2mg/ml doxycycline hyclate (Sigma) and 5mg/ml sucrose were added to the drinking water of the treatment groups, the control group received water with 5mg/ml sucrose only. Osimertinib (Tagrisso, AstraZeneca, 40 mg tablet) was dosed per os daily at a dose of 25mg/kg in Natrosol and control mice were dosed per os daily with Natrosol. To monitor side effects of treatment, mice were inspected daily for abnormalities and body weight was determined three times per week. Animals were sacrificed when the tumors reached a size of 1'500 mm³. Food and water were provided ad libitum. *In vivo* experiments were not repeated.

Immunohistochemistry

Xenograft samples were fixed in 4% formaldehyde for 24 h and embedded in paraffin. Two-micrometer-thick sections were cut using a microtome. STAG1 was stained with Polink 2 Plus HRP rat NM detection system (GBI Labs #D46-6) according to manufacturer's instructions using a recombinant rat monoclonal STAG1 antibody (Abcam ab241544, Lot:GR3334172-1; 1:200) after cooking 10 minutes at 110°C in antigen unmasking solution (Vector #H3301). After staining the slides were digitalized (scanner: Leica Aperio AT2). All slides were reviewed and evaluated for quality by a board-certified MD Pathologist.

Imaging analysis was performed using the digital pathology platform HALO (Indica Labs). A tissue-classifying algorithm was trained to selectively recognize viable tumor tissue against stroma, necrosis, and skin. The tissue classification output for each scan was reviewed and manually edited as necessary. A cell detection and scoring algorithm was trained to measure DAB optical density (OD) in the nuclei of tumor cells. A positivity threshold for DAB OD was determined by normalization with respect to the DAB OD as calculated from *bona fide* negative tissue (e.g., murine stroma as background). The object data for background-normalized nuclear ODs for each tumor cell were exported from three control and three doxycycline-treated cases (207945 and 33331 pooled objects, respectively). The cumulative distribution of the background-normalized DAB OD for each tumor cell nucleus was then plotted for control and doxycycline-treated cases, separately (supplemental figure 4, panel K).

Reagents, code and data availability

DNA sequences of the transgenes used in this study and the code used to generate the figures are available upon request. The workflow for the RNA-seq bioinformatics analyses is described in the Materials and Methods section. RNA sequencing data were uploaded to GEO with the accession numbers: GSE218404 and GSE218617. The data will be made publicly available upon acceptance of this manuscript. All ARTi cell lines and constructs described in this study are available upon request.

Cell lines

All newly generated ARTi cell lines are available upon request. The following parental cell lines were used:

Cell line name	species	Supplier name	Catalog number	Clone number
PC-9	human	ECACC	90071810	Lot# 14A030
MIA PaCa-2	human	ATCC	CRL-1420	Lot# 1350798
HT 1080	human	ATCC	CCL-121	Lot# 63835574
HCT 116	human	ATCC	CCL-247	Lot# 6028631
RKO	human	ATCC	CRL-2577	Lot# 59354083
MV4-11	human	ATCC	CRL-9591 (old number)	Lot# 58352230
MOLM-13	human	DSMZ	ACC 554	Lot# 11
NIH-3T3	human	ATCC	CRL-1658	Lot# 63292276
EPP2		KrasG12D, Trp53-/-, MYCOE PDAC cells (EPP2)	NA	NA

RN2	murine	MLL-AF9OE, NrasG12D AML cells (RN2; Zuber et al. 2011)	NA	NA
Gp2d	human	ECACC	95090714	Lot# 11E013
Ls513	human	ATCC	CRL-2134	Lot# 57761342
Ba/F3	murine	DSMZ	ACC300	
293T-Lenti-X	human	Clontech	632180	Lot# 1404558A

Competing interests

Alexandra Hörmann, Maja Corcokovic, Jasko Salkanovic, Fiona Spreitzer, Anna Köferle, Katrin Gitschtaler, Alexandra Popa, Sarah Oberndorfer, Nicole Budano, Jan G. Ruppert, Paolo Chetta, Melanie Wurm and Ralph Neumüller: Are or were full time employees Boehringer Ingelheim. Johannes Zuber: Quantro Therapeutics GmbH (Co-founder, Scientific Advisor, Shareholder); Mirimus Inc. (Scientific Advisor, Shareholder); AstraZeneca-CRUK Functional Genomics Consortium (Scientific Advisor); Boehringer Ingelheim (Research Support).

Funding

J.Z. is supported by the Swiss National Science Foundation (Early Postdoc Mobility Fellowship P2BSP3_188110) and European Union's Horizon 2020 research and innovation program under the Marie Skłodowska-Curie grant agreement No. 847548 (VIP2) and No. 101032582 (AML-SynergyX). Research at the IMP is supported by Boehringer Ingelheim and the Austrian Research Promotion Agency (Headquarter grant FFG-852936). MS is a member of the Boehringer Ingelheim Discovery Research global post-doc program.

Acknowledgements

The authors thank all colleagues in the labs of Johannes Z. and R.A.N. for critical discussions and technical support.

References

1. Mohr S. E. , Smith J. A. , Shamu C. E. , Neumüller R. A. , Perrimon N. (2014) **RNAi screening comes of age: improved techniques and complementary approaches** *Nat Rev Mol Cell Bio* **15**:591–600
2. Housden B. E. , et al. (2017) **Loss-of-function genetic tools for animal models: cross-species and cross-platform differences** *Nat Rev Genet* **18**:24–40
3. Jackson A. L. , et al. (2003) **Expression profiling reveals off-target gene regulation by RNAi** *Nat Biotechnol* **21**:635–637
4. Scacheri P. C. , et al. (2004) **Short interfering RNAs can induce unexpected and divergent changes in the levels of untargeted proteins in mammalian cells** *P Natl Acad Sci Usa* **101**:1892–1897

5. Lin X. , et al. (2005) **siRNA-mediated off-target gene silencing triggered by a 7 nt complementation** *Nucleic Acids Res* **33**:4527–4535
6. Fellmann C. , et al. (2013) **An Optimized microRNA Backbone for Effective Single-Copy RNAi** *Cell Reports* **5**:1704–1713
7. Premisrur P. K. , et al. (2011) **A Rapid and Scalable System for Studying Gene Function in Mice Using Conditional RNA Interference** *Cell* **145**:145–158
8. Zuber J. , et al. (2011) **Toolkit for evaluating genes required for proliferation and survival using tetracycline-regulated RNAi** *Nat Biotechnol* **29**:79–83
9. Vert J.-P. , Foveau N. , Lajaunie C. , Vandenbrouck Y. (2006) **An accurate and interpretable model for siRNA efficacy prediction** *Bmc Bioinformatics* **7**
10. Boudreau R. L. , et al. (2013) **siSPOTR: a tool for designing highly specific and potent siRNAs for human and mouse** *Nucleic Acids Res* **41**:e9–e9
11. Hynes N. E. , MacDonald G. (2009) **ErbB receptors and signaling pathways in cancer** *Curr Opin Cell Biol* **21**:177–184
12. Puneekar S. R. , Velcheti V. , Neel B. G. , Wong K.-K. (2022) **The current state of the art and future trends in RAS-targeted cancer therapies** *Nat Rev Clin Oncol* :1–19
<https://doi.org/10.1038/s41571-022-00671-9>
13. Bailey M. L. , et al. (2021) **Paralogous synthetic lethality underlies genetic dependencies of the cancer-mutated gene STAG2** *Life Sci Alliance* **4**
14. Lelij P. van der et al (2020) **STAG1 vulnerabilities for exploiting cohesin synthetic lethality in STAG2-deficient cancers** *Life Sci Alliance* **3**
15. Benedetti L. , Cereda M. , Monteverde L. , Desai N. , Ciccarelli F. D. (2014) **Synthetic lethal interaction between the tumour suppressor STAG2 and its paralog STAG1** *Oncotarget* **5**:37619–37632
16. Lelij P. van der et al (2017) **Synthetic lethality between the cohesin subunits STAG1 and STAG2 in diverse cancer contexts** *Elife* **6**
17. Fakih M. , et al. (2020) **CodeBreak 100: Activity of AMG 510, a novel small molecule inhibitor of KRAS G12C, in patients with advanced colorectal cancer** *J Clin Oncol* **38**:4018–4018
18. Lanman B. A. , et al. (2020) **Discovery of a Covalent Inhibitor of KRASG12C (AMG 510) for the Treatment of Solid Tumors** *J Med Chem* **63**:52–65
19. Fakih M. , et al. (2019) **Phase 1 study evaluating the safety, tolerability, pharmacokinetics (PK), and efficacy of AMG 510, a novel small molecule KRAS G12C inhibitor, in advanced solid tumors** *J Clin Oncol* **37**:3003–3003

20. Lai A. C. , Crews C. M. (2017) **Induced protein degradation: an emerging drug discovery paradigm** *Nat Rev Drug Discov* **16**:101–114
21. Cromm P. M. , Crews C. M. (2017) **Targeted Protein Degradation: from Chemical Biology to Drug Discovery** *Cell Chem Biol* **24**:1181–1190
22. Fellmann C. , et al. (2011) **Functional Identification of Optimized RNAi Triggers Using a Massively Parallel Sensor Assay** *Mol Cell* **41**:733–746
23. Galla M. , et al. (2011) **Avoiding cytotoxicity of transposases by dose-controlled mRNA delivery** *Nucleic Acids Res* **39**:7147–7160
24. Yang W. , et al. (2013) **Genomics of Drug Sensitivity in Cancer (GDSC): a resource for therapeutic biomarker discovery in cancer cells** *Nucleic Acids Res* **41**:D955–D961
25. Smith T. , Heger A. , Sudbery I. (2017) **UMI-tools: modeling sequencing errors in Unique Molecular Identifiers to improve quantification accuracy** *Genome Res* **27**:491–499
26. Martin M. (2011) **Cutadapt removes adapter sequences from high-throughput sequencing reads** *Embnet J* **17**:10–12
27. Neumann T. , et al. (2019) **Quantification of experimentally induced nucleotide conversions in high-throughput sequencing datasets** *Bmc Bioinformatics* **20**
28. Muhar M. , et al. (2018) **SLAM-seq defines direct gene-regulatory functions of the BRD4-MYC axis** *Science* **360**:800–805
29. Liao Y. , Smyth G. K. , Shi W. (2014) **featureCounts: an efficient general purpose program for assigning sequence reads to genomic features** *Bioinformatics* **30**:923–930
30. Love M. I. , Huber W. , Anders S. (2014) **Moderated estimation of fold change and dispersion for RNA-seq data with DESeq2** *Genome Biol* **15**
31. Dobin A. , et al. (2013) **STAR: ultrafast universal RNA-seq aligner** *Bioinformatics* **29**:15–21
32. Li B. , Dewey C. N. (2011) **RSEM: accurate transcript quantification from RNA-Seq data with or without a reference genome** *Bmc Bioinformatics* **12**
33. Ritchie M. E. , et al. (2015) **limma powers differential expression analyses for RNA-sequencing and microarray studies** *Nucleic Acids Res* **43**:e47–e47
34. Law C. W. , Chen Y. , Shi W. , Smyth G. K. (2014) **voom: precision weights unlock linear model analysis tools for RNA-seq read counts** *Genome Biol* **15**:R29–R29
35. Wilding B. , et al. (2022) **Discovery of potent and selective HER2 inhibitors with efficacy against HER2 exon 20 insertion-driven tumors, which preserve wild-type EGFR signaling** *Nat Cancer* **3**:821–836

36. Li D. , et al. (2008) **BIBW2992, an irreversible EGFR/HER2 inhibitor highly effective in preclinical lung cancer models** *Oncogene* **27**:4702–4711
37. Liu S. , et al. (2018) **Targeting HER2 Aberrations in Non-Small Cell Lung Cancer with Osimertinib** *Clin Cancer Res* **24**:2594–2604
38. Soria J.-C. , et al. (2018) **Osimertinib in Untreated EGFR -Mutated Advanced Non-Small-Cell Lung Cancer** *New Engl J Med* **378**:113–125
39. Kim T.-Y. , et al. (2019) **A phase I/II study of poziotinib combined with paclitaxel and trastuzumab in patients with HER2-positive advanced gastric cancer** *Gastric Cancer* **22**:1206–1214
40. Robichaux J. P. , et al. (2019) **Pan-Cancer Landscape and Analysis of ERBB2 Mutations Identifies Poziotinib as a Clinically Active Inhibitor and Enhancer of T-DM1 Activity** *Cancer Cell* **36**:444–457

Author information

Thomas Hoffmann

Institute of Molecular Pathology (IMP), Campus-Vienna-Biocenter 1, 1030 Vienna, Austria, Vienna BioCenter PhD Program, Doctoral School of the University at Vienna and Medical University of Vienna, Vienna BioCenter (VBC), 1030 Vienna, Austria, Advantage Therapeutics GmbH, Karl-Farkas-Gasse 22, 1030 Vienna, Austria
ORCID iD: [0000-0002-1589-0013](https://orcid.org/0000-0002-1589-0013)

Alexandra Hörmann

Boehringer Ingelheim RCV GmbH & Co KG, Doktor-Boehringer-Gasse 5-11, 1120 Vienna, Austria

Maja Corcokovic

Boehringer Ingelheim RCV GmbH & Co KG, Doktor-Boehringer-Gasse 5-11, 1120 Vienna, Austria

Jakub Zmajkovic

Institute of Molecular Pathology (IMP), Campus-Vienna-Biocenter 1, 1030 Vienna, Austria

Matthias Hinterndorfer

Institute of Molecular Pathology (IMP), Campus-Vienna-Biocenter 1, 1030 Vienna, Austria
ORCID iD: [0000-0003-2435-4690](https://orcid.org/0000-0003-2435-4690)

Jasko Salkanovic

Boehringer Ingelheim RCV GmbH & Co KG, Doktor-Boehringer-Gasse 5-11, 1120 Vienna, Austria

Fiona Spreitzer

Boehringer Ingelheim RCV GmbH & Co KG, Doktor-Boehringer-Gasse 5-11, 1120 Vienna, Austria

Anna Köferle

Boehringer Ingelheim RCV GmbH & Co KG, Doktor-Boehringer-Gasse 5-11, 1120 Vienna, Austria

ORCID iD: [0000-0003-1601-7774](https://orcid.org/0000-0003-1601-7774)

Katrin Gitschtaler

Boehringer Ingelheim RCV GmbH & Co KG, Doktor-Boehringer-Gasse 5-11, 1120 Vienna, Austria

Alexandra Popa

Boehringer Ingelheim RCV GmbH & Co KG, Doktor-Boehringer-Gasse 5-11, 1120 Vienna, Austria

Sarah Oberndorfer

Boehringer Ingelheim RCV GmbH & Co KG, Doktor-Boehringer-Gasse 5-11, 1120 Vienna, Austria

Florian Andersch

Institute of Molecular Pathology (IMP), Campus-Vienna-Biocenter 1, 1030 Vienna, Austria

Markus Schäfer

Institute of Molecular Pathology (IMP), Campus-Vienna-Biocenter 1, 1030 Vienna, Austria

Michaela Fellner

Institute of Molecular Pathology (IMP), Campus-Vienna-Biocenter 1, 1030 Vienna, Austria

Nicole Budano

Boehringer Ingelheim RCV GmbH & Co KG, Doktor-Boehringer-Gasse 5-11, 1120 Vienna, Austria

Jan G. Ruppert

Boehringer Ingelheim RCV GmbH & Co KG, Doktor-Boehringer-Gasse 5-11, 1120 Vienna, Austria

Paolo Chetta

Boehringer Ingelheim RCV GmbH & Co KG, Doktor-Boehringer-Gasse 5-11, 1120 Vienna, Austria

Melanie Wurm

Boehringer Ingelheim RCV GmbH & Co KG, Doktor-Boehringer-Gasse 5-11, 1120 Vienna, Austria

Johannes Zuber

Institute of Molecular Pathology (IMP), Campus-Vienna-Biocenter 1, 1030 Vienna, Austria, Medical University of Vienna, Vienna BioCenter, 1030 Vienna, Austria

For correspondence: johannes.zuber@imp.ac.at

ORCID iD: [0000-0001-8810-6835](https://orcid.org/0000-0001-8810-6835)

Ralph A. Neumüller

Boehringer Ingelheim RCV GmbH & Co KG, Doktor-Boehringer-Gasse 5-11, 1120 Vienna, Austria

For correspondence: ralph.neumueller@boehringer-ingelheim.com

ORCID iD: [0000-0002-1514-6278](https://orcid.org/0000-0002-1514-6278)

Editors

Reviewing Editor

Michael Eisen

University of California, Berkeley, United States of America

Senior Editor

Michael Eisen

University of California, Berkeley, United States of America

Reviewer #1 (Public Review):

In this manuscript the authors proposed a novel system by which they can suppress the expression of any gene of interest precisely and efficiently with a pre-validated, highly specific and efficient synthetic short-hairpin RNA. The idea of identifying potent artificial RNAi (ARTi) triggers is intriguing, and the authors successfully identify six ARTi with robust knockdown efficiency and limited to no off-target effects. As a proof-of-concept, the authors examined three oncology targets for validation, including EGFRdel19 (which already has a clinically approved drug for validation), KRASG12R (for which there are no in vivo compatible inhibitors yet) and STAG1 (which has a synthetic lethal interaction with recurrent loss-of-function mutations of STAG2). The authors demonstrated significant suppression of colony formation and in vivo tumor growth for all three oncology targets.

This novel system could serve as a powerful tool for loss-of-function experiments that are often used to validate a drug target. Not only this tool can be applied in exogenous systems (like EGFRdel19 and KRASG12R in this paper), the authors successfully demonstrated that ARTi can also be used in endogenous systems by CRISPR knocking in the ARTi target sites to the 3'UTR of the gene of interest (like STAG2 in this paper).

ARTi enables specific, efficient, and inducible suppression of these genes of interest, and can potentially improve therapeutic target validations. However, the system cannot be easily generalized as there are some limitations in this system:

- The authors claim in the introduction that CRISPR/Cas9-based methods are associated with off-target effects, however, the author's system requires the use CRISPR/Cas9 to knock out a given endogenous genes or to knock-in ARTi target sites to the 3' UTR of the gene of interest. Though the authors used a transient CRISPR/Cas9 system to minimize the potential off-target effects, the methods does not, as the authors acknowledge, eliminate the possibility of off-target effects.
- Instead of generating gene-specific loss-of-function triggers for every new candidate gene, the authors identified a universal and potent ARTi to ensure standardized and controllable knockdown efficiency. It seems this would save time and effort in validating each lost-of-function siRNAs/sgRNAs for each gene. However, users will still have to design and validate the best sgRNA to knock out endogenous genes or to knock in ARTi target sites by

CRISPR/Cas9. The latter is by no-means trivial. Users will need to design and clone an expression construct for their cDNA replacement construct of interest, which will still be challenging for big proteins. This is not, as the authors point out, a replacement for other LOF methods, and there are other ways to achieve gene-specific regulation via, for example, degrons. However it is an effective orthogonal approach that many users may find compelling for their applications.

Reviewer #2 (Public Review):

In this manuscript, Hoffmann et al. introduce a novel and innovative method to validate and study the mechanism of action of essential genes and novel putative drug targets. In the wake of many functional genomics approaches geared towards identifying novel drug targets or synthetic lethal interactions, there is a dire need for methods that allow scientists to ablate a gene of interest and study its immediate effect in culture or in xenograft models. In general, these genes are lethal, rendering conventional genetic tools such as CRISPR or RNAi inept.

The ARTi system is based on expression of a transgene with an artificial RNAi target site in the 3'-UTR as well as a TET-inducible miR-E-based shRNAi. Using this system, the authors convincingly show that they can target strong oncogenes such as EGFRdel19 or KRasG12 as well as synthetic lethal interactions (STAG1/2) in various human cancer cell lines in vivo and in vitro.

The system is very innovative, likely easy to be established and used by the scientific community and thus very meaningful.

Author Response:

The following is the authors' response to the original reviews.

Reviewer #1 (Public Review):

[...] This novel system could serve as a powerful tool for loss-of-function experiments that are often used to validate a drug target. Not only this tool can be applied in exogenous systems (like EGFRdel19 and KRASG12R in this paper), the authors successfully demonstrated that ARTi can also be used in endogenous systems by CRISPR knocking in the ARTi target sites to the 3'UTR of the gene of interest (like STAG2 in this paper).

We thank the referee for highlighting the novelty and potential of the ARTi system.

ARTi enables specific, efficient, and inducible suppression of these genes of interest, and can potentially improve therapeutic target validations. However, the system cannot be easily generalized as there are some limitations in this system:

- The authors claimed in the introduction sections that CRISPR/Cas9-based methods are associated with off-target effects, however, the author's system requires the use CRISPR/Cas9 to knock out a given endogenous genes or to knock-in ARTi target sites to the 3' UTR of the gene of interest. Though the authors used a transient CRISPR/Cas9 system to minimize the potential off-target effects, the advantages of ARTi over CRISPR are likely less than claimed.*

We thank the reviewer for raising these very valid concerns about potential off-target effects related to the CRISPR/Cas9-based gene knockout or engineering of endogenous ARTi target sites. In contrast to conventional RNAi- and CRISPR-based approaches, such off-target effects

can be investigated prior to loss-of-function experiments through comparison between parental and engineered cells, which in the absence of CRISPR-induced off-target events are expected to be identical. Subsequent ARTi experiments provide full control over RNAi-induced off-target activities through comparison of target-site engineered and parental cells. However, we agree that undetected CRISPR/Cas9-induced off-target events cannot be ruled out in a definitive way, which we have pointed out in our revised manuscript.

• Instead of generating gene-specific loss-of-function triggers for every new candidate gene, the authors identified a universal and potent ARTi to ensure standardized and controllable knockdown efficiency. It seems this would save time and effort in validating each lost-of-function siRNAs/sgRNAs for each gene. However, users will still have to design and validate the best sgRNA to knock out endogenous genes or to knock in ARTi target sites by CRISPR/Cas9. The latter is by no-means trivial. Users will need to design and clone an expression construct for their cDNA replacement construct of interest, which will still be challenging for big proteins.

We fully agree that the required design of gene-specific sgRNAs and subsequent CRISPR-engineering steps are by no means trivial. However, we believe that decisive advantages of the method, in particular the robustness of LOF perturbations and additional means for controlling off-target activities, can make ARTi an investment that pays off. In our experience, much time can be lost in the search for effective LOF reagents, and even when these are found, questions about off-target activity remain. While ARTi overcomes many of these challenges by providing a standardized experimental workflow, we do not propose to replace all other LOF approaches by this method. Instead, we would position ARTi as a unique orthogonal approach for the stringent validation and in-depth characterization of candidate target genes, as we have highlighted in our revised discussion.

• The approach of knocking-out an endogenous gene followed by replacement of a regulatable gene can also be achieved using regulated degrons, and by tet-regulated promoters included in the gene replacement cassette. The authors should include a discussion of the merits of these approaches compared with ARTi.

We thank the reviewer for pointing out these alternative LOF methods. We had already included a brief discussion of chemical-genetic LOF methods based on degron tags. While we certainly share the current excitement about degron technologies, they inevitably require changes to the coding sequence of target proteins, which can alter their regulation and function in ways that are hard to control for. In our revised discussion, we have added a brief comparison to conventional tet-regulatable expression systems, which unlike ARTi require the use of ectopic tet-responsive promoters. Overall, we would position ARTi as an orthogonal tool that enables inducible and reversible LOF perturbations without changing the coding sequence and the endogenous transcriptional control of candidate target genes.

Reviewer #2 (Public Review):

[...] The ARTi system is based on expression of a transgene with an artificial RNAi target site in the 3'-UTR as well as a TET-inducible miR-E-based shRNAi. Using this system, the authors convincingly show that they can target strong oncogenes such as EGFRdel19 or KRasG12 as well as synthetic lethal interactions (STAG1/2) in various human cancer cell lines in vivo and in vitro.

The system is very innovative, likely easy to be established and used by the scientific community and thus very meaningful.

We thank the reviewer for her/his enthusiasm about ARTi.

Reviewer #1 (Recommendations For The Authors):

• The authors claimed that ARTi enables specific, efficient, inducible, and reversible suppression of any gene of interest. However, there are no experiments supporting the reversible suppression of their gene of interest. Data are required to support this statement.

We thank the reviewer for pointing this out. The statement about the reversibility ARTi-mediated effects was based on a rich body of literature that has demonstrated the reversibility of Tet-shRNAmir-induced LOF perturbations and associated phenotypes. As ARTi employs the same Tet-shRNAmir expression vectors, we have no reason to believe that this feature would be lost. However, since we have not demonstrated this in our study, we have removed this statement in our revised manuscript.

• In Figure 1E, the authors did make the point by including trametinib treated samples as positive controls. However, the trametinib treated samples also made the transcriptome changes in the ARTi groups hard to read. I wonder what the PCA analysis will look like if the authors exclude the trametinib treated groups.

In Figure 1E, we used PCA as a common and easy-to-digest visualization tool to showcase the neutrality of ARTi shRNAmirs. Given the complete absence of significantly deregulated genes for all three ARTi shRNAmirs (Figure 1F), we believe that a PCA analysis of just these samples would merely represent experimental noise and not yield additional insights.

• This universal and potent ARTi should ensure standardized and controllable knockdown efficiency, however, the knockdown efficiency for KRASG12R is not as potent as that for EGFRdel19. The authors should discuss the differences.

We thank the reviewer for pointing this out. The exact level of knockdown on the protein level is hard to determine due to detection limits of the used method. The differences in the extent to mRNA knockdown could be attributable to cleavage efficiencies due to potential secondary structures in the respective mRNAs. We suspect that the KRASG12R transgene expresses at higher levels, compared to EGFRdel19. We might therefore still be looking at the same overall magnitude of knockdown. As we did not perform a detailed analysis of the respective knockdown levels, we do not feel comfortable in stating differences in knockdown levels and therefore do not think that addressing potential differences are justified.

• It is interesting to see that, unlike other cancer types, tumor burdens did not decrease after inducing knockdown of STAG1 in STAG2 knockout HCT116 lines in Figure 2L. Have the authors examined senescence markers in this set of mice?

We have not investigated these markers and thank the reviewer for this suggestion. More detailed analyses of the phenotype are planned.

• Have the authors carefully examined the transcriptome changes induced or if not across all targets at least in the case of ARTi knock into the 3'UTR of STAG1?

We thank the reviewer for this suggestion. This would indeed be interesting to conduct for STAG1/2, especially for genes with an integration of the ARTi into the 3'UTR. The reason why we did not perform this analysis with our cell lines is that we used a construct that also adds an AID tag to STAG1 (STAG1_AID_V5_P2A_Blasti_STOP_ARTi), as outlined in the methods section. After the engineering, STAG1 carries the ARTi sequence in the 3'UTR but is also fused to AID::V5. In addition a P2A::Blasticidin_resistance Protein is made from the same transcript. We chose to use this complex strategy with the aim of comparing AID mediated degradation with ARTi-mediated knockdown. Unfortunately, the AID-based approach did not work, and we were not able to observe a reduction in protein levels. We however observed lower expression of STAG1 in the engineered versus the parental cells, likely caused by the tag, and

consequently did not conduct gene expression analyses, as we would not be able to assess if transcriptome changes could be solely ascribed to the changes in the 3'UTR. The knockdown levels are hence only analyzed on the protein level.

Reviewer #2 (Recommendations For The Authors):

This is a fantastic paper, easy to read and provides a very meaningful new and innovative approach for drug target validation. I think the manuscript could be further improved by adding a section to the discussion outlining other approaches that could be used to solve the same problem. For example, Bill Kaelin came up with a strategy of expressing shRNA- or sgRNA-resistant and rtTA- or tTA-regulated cDNAs of essential gene-of-interest followed by sh/sgRNA-mediated ablation of the endogenous gene (e.g. PMID: 28082722), which is conceptually quite similar to the ARTi approach. Similarly, people have used conditional degron tags such as AID tags, dTags, HALOTags, IZH3F3 degrons or SMASh either knocked into the endogenous locus or as rescue transgene. Comparing and contrasting the pros and cons of these methods to the ARTi-based approach would be certainly beneficial to the readers.

We thank the referee for pointing out these alternative LOF methods. We certainly share the current excitement about various degron tags and are applying them in our own research. In our view, a major downside of these strategies is that they inevitably require changes to the coding sequence of target proteins, which can alter their regulation and function in ways that are hard to predict and control for. We had briefly mentioned this distinguishing feature in our discussion. The strategy proposed by Bill Kaelin, i.e. rescue of the the endogenous gene through Tet-regulated expression of sh/sgRNA-resistant cDNAs, indeed shares many features of the ARTi system, but requires expression of the candidate target from an ectopic promoter element. In contrast, ARTi enables similar perturbations of candidate genes without altering their endogenous transcriptional regulations – a feature that we have highlighted in our revised discussion.

All my other comments outlined below should be considered minor and are not essential.

1, Suppl Fig.1 C: Please explain what the red star means. How can the knock-out be more than 100%. Please specify what the controls are. Why does shRNA660 exhibit no knockdown at all?

The red star indicates ARTi-shRNAmirs that were selected for further characterization. Depicted GFP knockdown levels are normalized to the performance of shRen.713, a well-characterized potent control shRNA targeting Renilla Luciferase. Values of more than 100% mean that the respective shRNA exceeded effects of shRNA.713. shRNA.660 served as a neutral control – its target site was not included in the reporter construct. We thank the reviewer for bringing up these points, which we have clarified in the legend.

2, x-axis label in Suppl Fig. 1D is missing

We thank the referee for spotting this and have added this information to the figure and its legend.

3, I would argue that ARTi6634 also has a slight effect in MV4-11 similar to its effect to RN2. Maybe add that to the text.

We thank the reviewer and have added this observation to our revised text.

4, Suppl. Figure Legend 1F - specify which cell line was used (HT-1080 presumably)

We apologize for this mistake and now have indicated the cell line in the legend.

5, Fig. 2A and E, it might be nice to add the dsRED fusion to the schematics so that the reader sees the difference between the endogenous and the endogenous. One could then also change the color to red instead of blue.

We thank the reviewer for this suggestion and adapted the figure accordingly.

6, Fig. 2B - In the third lane, there appears to be a residual band of the endogenous EGFR despite the fact that it should be KO. Is this a EGFR wt lysate with EGFR::dsRED::ARTi overexpression and as such a type in the legend or is this a non-complete KO? It might be beneficial to label the legend with EGFR::dsRED::ARTi instead of EGFR::ARTi have one arrow depicting EGFR and one additional arrow showing the EGFR::dsRED fusion (as in Fig. 1F).

We thank the reviewer for this insightful comment. We interpret the WB signal in lane three as potential cleavage/degradation products of the transgene as all signal disappears upon ARTi-mediated knockdown. Due to space reasons, we would prefer to keep the label as it is. The exact nature of the transgene is stated in the text and in the methods section.

7, Suppl Fig. 2d: It is interesting that there is such a huge upregulation of DUSP6 in cells that express EGFR::ARTi compared to parental? The figure legend states: expression levels of DUSP6 in parental and engineered PC-9 cells. I assume the first box (EGFR::ARTi -/ dox -) is the parental line? Is there really a 5x upregulation of DUSP6 upon overexpression of EGFR::ARTi compared to parental (despite the fact that the endogenous EGFR::ARTi is expressed to similar levels compared to the endogenous EGFR)? Please clarify a little better which of the cells are parental and which are EGFR KO and which are transduced with EGFR::ARTi. Might suffice to just explain in the supplemental figure legend that expression of the exogenous EGFR::ARTi in EGFR KO cells leads to increased expression of ERK targets such as DUSP6 and EPHA2 etc.

We thank the reviewer for this comment. We ascribe the increased expression of DUSP6 to the forced expression of the oncogenic variant of EGFR (EGFRdel19) while only a subset of *EGFR* genes in PC-9 cells is mutated and the rest is wild-type. Therefore, the net-output of EGFR signaling would be higher, even if the EGFR protein levels were exactly the same, as the *EGFR* gene is only present in the oncogenic form in the engineered cells but a mixture of mutant and wild-type proteins would make up the EGFR pool in the parental cells. The figure legend was changed accordingly, highlighting that *DUSP6* is a MAPK downstream gene.

8, Suppl Fig. 2e: Similar to my comment #7. Expression of endogenous EGFR is lost upon KO of EGFR, but cyclinD1 expression as well as expression of other ERK target genes increases upon loss of the endogenous EGFR gene with concomitant expression of EGFR::ARTi. It is nice to see that most of those genes are down-regulated upon DOX treatment. However, CyclinD1 is strongly up-regulated - any idea why? Might be nice to comment on this in the supplemental material to make it easy for the reader to interpret the data.

We agree with the reviewer that the direct MAPK target genes follow the expected pattern of strong downregulation. We have not studied the expression of *CCND1* in detail and therefore cannot comment on the mechanistic basis of this observation.

9, Fig. 2F - might be nice to provide some densitometry data to quantify the effect of ARTi-mediated KRasG12R knock-down.

We thank the reviewer for this suggestion and apologize that this data is not available for this study. We will include densitometry data in upcoming studies involving ARTi. As the observed knockdown was almost complete and hence readily observable by eye, we did not measure the effects using densitometry. In addition, we would like to mention that the sensor assay contains a quantitative analysis of the knockdown levels.

10, Fig. 2I, it might be nice to add the V5 tag to the schematic and mention the V5 tag in the text: ... and homozygously inserted ARTi target sites into the 3'-UTR as well as a V5 tag to the endogenous STAG1 alleles (Fig. 2i)

We thank the reviewer for the suggestion and explained the exact makeup of the construct better in the main text. We would however like to keep the figure as simple as possible and put the focus on the endogenous engineering here.

11, Fig. 2J - might be nice to provide some densitometry data to quantify the effect of ARTi-mediated STAT1::V5 knock-down.

We thank the reviewer for this suggestion and apologize that this data is not available for this study. We will include densitometry data in upcoming studies involving ARTi. As the observed knockdown was almost complete and hence readily observable by eye, we did not measure the effects using densitometry. In addition, we would like to mention that the sensor assay contains a quantitative analysis of the knockdown levels.

12, Suppl. Fig 4B: the authors write: 'Western blotting confirmed ... the homozygous insertion of the targeting cassette into the STAG1 locus, ...'. I think the WB nicely shows insertion of the V5 tag into the STAG1 locus, but it I think WB cannot show homozygous insertion. The fact that in Suppl Fig 1B STAG1 expression is (almost) completely ablated, is a good indication, but in Fig. 2J, there is still about 50% expression. As such, proofing homozygous insertion by PCR/Sanger sequencing or densitometry over several experiments or just rephrasing the text a little might be beneficial.

We agree with the reviewer and have adapted the respective passage in the main text.

Competing interests statement: A patent application related to the design and use of the ARTi system entitled 'Methods and molecules for RNA interference (RNAi)' has been submitted by T.H., M.H., J.Z. and R.N. to the European Patent Office (application EP21217407.2).